

iSAGE: An Incremental Version of SAGE for Online Explanation on Data Streams

Maximilian Muschalik ^{*1,2} Fabian Fumagalli ^{*3} Barbara Hammer ³ Eyke Hüllermeier ^{1,2}

Abstract

Explainable Artificial Intelligence (XAI) focuses mainly on batch learning scenarios. In the static learning tasks, various XAI methods, like SAGE, have been proposed that distribute the importance of a model on its input features. However, models are often applied in ever-changing dynamic environments like incremental learning. As a result, we propose iSAGE as a direct incrementalization of SAGE suited for dynamic learning environments. We further provide an efficient approximation method to model feature removal based on the conditional data distribution in an incremental setting. We formally analyze our explanation method to show that it is an unbiased estimator and construct confidence bounds for the point estimates. Lastly, we evaluate our approach in a thorough experimental analysis based on well-established data sets and concept drift streams.

1. Introduction

Data streams are encountered in various machine learning applications, such as online credit risk scoring for financial services (Clements et al., 2020), intrusion detection in networks (Atli & Jung, 2018), or sensor network analysis (Bahri et al., 2021). In applications of that kind, online learning from data streams is required to be time- and memory-efficient. More importantly, incremental models also need to account for shifts in the underlying data distribution, which is referred to as *concept drift*. Such drift may occur in different forms and for different reasons, e.g., as a change of energy consumption patterns or hospital admission criteria due to pandemic-induced lockdowns (Duckworth et al., 2021). All types of unaddressed concept drift may affect the modeling performance.

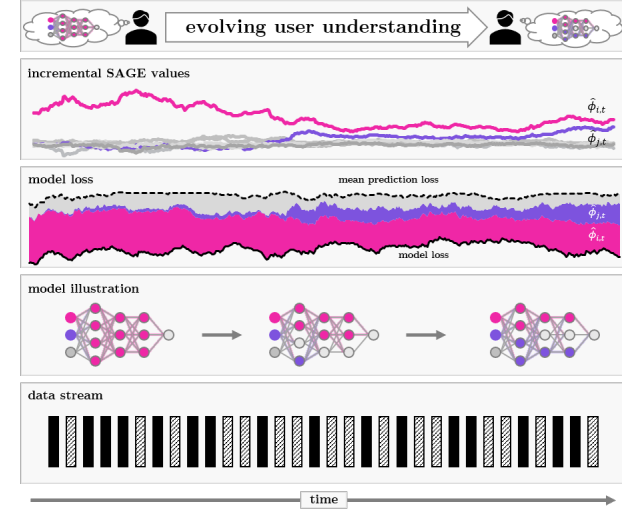


Figure 1: An incremental model learns from samples of a data stream. Incrementally explaining this model with iSAGE efficiently distributes the FI scores according to the model’s loss evolving the user understanding of the model.

If machine learning models are used for high-stake decision-making, e.g., in healthcare (Ta et al., 2016) or energy consumption analysis (García-Martín et al., 2019), these models should be transparent and explainable. The field of explainable artificial intelligence (XAI) emerged as a solution to uncover the inner working of black box models (Adadi & Berrada, 2018). High-performance models are often opaque in nature, making input-output relationships difficult to understand. XAI approaches categorized as *global feature importance* (global FI) methods quantify the dependence of a model on its input features. FI measures seek to rank features of a model in terms of their importance.

So far, XAI has mainly focused on static learning scenarios and mostly neglected important challenges of online learning. However, in dynamic scenarios, where models are constantly evolving and reacting to their changing environment, static explanations are no longer enough. Instead, explanations for monitoring dynamic models need to be updated in a continuous manner, just like the models themselves. For example, we could be interested in computing

^{*}Equal contribution ¹LMU Munich, D-80539 Munich, Germany

²Munich Center for Machine Learning (MCML) ³Bielefeld University, D-33615 Bielefeld, Germany. Correspondence to: Maximilian Muschalik <Maximilian.Muschalik@ifi.lmu.de>, Fabian Fumagalli <ffumagalli@techfak.uni-bielefeld.de>.

global FI in an incremental manner, thereby also addressing the challenge of drifting data distributions. This quest comes with various challenges, not only conceptually and algorithmically but also computationally, especially because the computation of many FI measures is already prohibitive in the batch setting.

Contribution. Our main contributions include:

- *iSAGE*; a novel *model-agnostic, global* FI method for dynamic learning environments that directly incrementally realizes the well-known SAGE algorithm,
- a formal analysis of iSAGE in terms of its expectation and construction of δ -confidence bounds,
- *incremental, conditional feature removal*; an efficient feature removal technique that more closely approximates the conditional data distribution compared to the marginal data distribution.
- *open source implementation*; a well-tested and general implementation¹ of our algorithms and experiments that integrates into the well-known *River* (Montiel et al., 2021) Python framework.

Related Work. Global FI is an active part of XAI research, and various methods have been proposed. Permutation Feature Importance (PFI) (Breiman, 2001) is a well-established model-agnostic, global FI method that was recently extended to function differently when features are correlated (Molnar et al., 2020). One of PFI’s main limitations is that features are evaluated individually, and the impact of differently sized feature subsets is not considered. Different approaches have been proposed to address this limitation (Casalicchio et al., 2019; König et al., 2021) including SAGE (Covert et al., 2020). SAGE can be understood as an efficient approximation of the Shapley value (Shapley, 1953) for ML, similar to SHAP (Lundberg & Lee, 2017) and LossSHAP (Lundberg et al., 2020). It is based on a permutation-based sampling algorithm Castro et al. (2009).

To calculate the importance of different feature subsets, SAGE requires knowledge about the underlying data distribution (Covert et al., 2020; 2021). SAGE, in its original definition, relies on the conditional data distribution, which is approximated by the marginal data distribution in practice (Covert et al., 2020). The conditional subgroup approach for PFI (Molnar et al., 2020) efficiently approximates the conditional data distribution by inducing tree models. Other, computationally more expensive methods like SHAPr by Aas et al. 2021, approximate the underlying data distribution

directly for Shapley-based explanation methods (Chen et al., 2020; Frye et al., 2021). Yet, due to their computational overhead, they may be unsuited for incremental learning.

Traditionally, XAI focuses on the batch learning scenario. However, recently more methods that natively support incremental, dynamic learning environments are proposed. Haug et al. 2022 propose a concept drift detection algorithm based on clusterings and changes in SHAP’s mean-prediction. A model-specific approach for tree-based models is measuring the mean decrease in impurity (Cassidy & Deviney, 2014). In the notion of explaining change (Muschalik et al., 2022), iPFI (Fumagalli et al., 2022) is a related model-agnostic approach that computes the traditional yet in the context of feature dependencies suboptimal PFI (Breiman, 2001) in an incremental manner. Since FI closely relates to feature selection, online feature selection methods are proposed that compute FI periodically (Barddal et al., 2019; Yuan et al., 2018).

2. Shapley Additive Global Importance (SAGE)

Covert et al. 2021 introduce *removal-based explanations* as a unified framework that summarizes many existing popular feature attribution methods in XAI, such as SHAP, LIME (Ribeiro et al., 2016), SAGE, IME (Zeiler & Fergus, 2014), and PFI. Removal-based explanations compare the change in a model’s behavior, such as the loss or a prediction, when features are removed from the model’s input. The difference in the model’s behavior measured when restricting to a feature subset $S \subset D$ is called *marginal contribution* of S . Each explanation method can then be characterized by the following three key components:

- **Feature Removal:** Given a model f , how to compute a restricted model f^S for subsets $S \subset D$, e.g. by using default values, marginalizing features or retraining it?
- **Model Behavior:** Given a restricted model f^S , what constitutes the characteristic function ν^f to explain? In particular, what is the value of interest $\nu^f(D)$ to explain the model behavior, e.g. the probability of the true class (local) or the dataset loss (global).
- **Summary Technique:** Given the characteristic function ν^f , how to aggregate a feature’s marginal contribution among different subsets, e.g. computing a Shapley value or relying on specific combinations of subsets?

In the following, we describe SAGE as an instantiation of this framework. SAGE, as a global FI measure, aims to explain the difference in the dataset loss and the loss of a model that uses no feature information. Marginal contributions of feature subsets are computed using a restricted

¹iSAGE is implemented as part of *iXAI* and publicly available at <https://github.com/mmschlk/iXAI>.

model based on marginalization as a feature removal technique. As a summary technique, the marginal contributions of each feature among all feature subsets are aggregated to compute the Shapley value.

Feature Removal Given a model f , the restriction of subsets in SAGE is defined as

$$f^S(x) := \mathbb{E}_{\tilde{X} \sim p}[f(x^{(S)}, \tilde{X})], \quad (1)$$

where $p := \mathbb{P}(X^{(\bar{S})} | X^{(S)} = x^{(S)})$ is the conditional distribution that depends on S , and $x^{(S)} := (x^{(i)} : i \in S)$ are the features of x with indices in S . Thus, f^S only considers the features of x which are in S and averages over the remaining. The values of $f^S(x)$ are inaccessible in practice but can be approximated by $\hat{f}^S(x) := \frac{1}{M} \sum_{m=1}^M f(x^{(S)}, x_m^{(\bar{S})})$ with $\bar{S} := D \setminus S$ using inputs \tilde{x}_m sampled according to an accessible distribution $q \approx p$. The SAGE algorithm proposes the marginal distribution $q := q(X^{(\bar{S})} | X^{(S)} = x^{(S)}) := \mathbb{P}(X^{(\bar{S})})$, which corresponds to p in case of feature independence (Covert et al., 2020). Related methods estimate p directly (Aas et al., 2021; Chen et al., 2020; Frye et al., 2021) or rely directly on the marginal distribution for p (Casalicchio et al., 2019), which has been discussed as the conceptually right choice (Janzing et al., 2020).

Model Behavior - Data set Loss To attribute global importance values, SAGE relies on the *reduction in risk* over the mean prediction as features are marginalized, i.e.

$$\nu^f(S) := \overbrace{\mathbb{E}_{(X,Y)}[\mathcal{L}(f^\emptyset(X^\emptyset), Y)] -}^{\text{mean prediction loss}} \overbrace{\mathbb{E}_{(X,Y)}[\mathcal{L}(f^S(X^{(S)}), Y)]}^{\text{marginalized loss over } p},$$

where $f^S(\cdot)$ is a restricted model, further specified below, and $\mathcal{L}(\cdot)$ a suitable loss function. SAGE aims to quantify the individual feature's contributions on the difference between the model's dataset loss compared with the mean prediction loss, i.e.

$$\hat{\nu}^f(D) = \frac{1}{N} \sum_{n=1}^N [\mathcal{L}(f^\emptyset(x_n), y_n) - \mathcal{L}(f(x_n), y_n)] \approx \nu^f(D),$$

and $\hat{\nu}^f(S) := \frac{1}{N} \sum_{n=1}^N [\mathcal{L}(f^\emptyset(x_n), y_n) - \mathcal{L}(f^S(x_n), y_n)]$ is the empirical approximation of $\nu^f(S)$.

Summary Technique - Shapley Value SAGE uses the Shapley value as its summary technique. The Shapley value is a concept from cooperative game theory. Given a set D of d players and a *characteristic* function ν specifying a value $\nu(S)$ for every subset of players $S \subset D$, the Shapley value is the unique value that attributes a payout $\phi^\nu(i)$ to

each player $i \in D$ by computing a weighted average over all marginal player contributions

$$\phi^\nu(i) := \sum_{S \subset D \setminus \{i\}} \frac{1}{d} \binom{d-1}{|S|}^{-1} [\nu(S \cup \{i\}) - \nu(S)].$$

It was shown that the Shapley value is the unique solution, such that meaningful axioms are fulfilled, in particular the *efficiency* property $\sum_{i \in D} \phi^\nu(i) = \nu(D) - \nu(\emptyset)$ (Shapley, 1953). Due to its exponential complexity, different approximation methods for the Shapley value have been proposed. A popular sampling-based approach (Castro et al., 2009) makes use of the alternative characterization

$$\begin{aligned} \phi^\nu(i) &= \frac{1}{d!} \sum_{\pi \in \mathfrak{S}_D} \nu(u_i^-(\pi)) - \nu(u_i^+(\pi)) = \\ &= \mathbb{E}_{\varphi \sim \text{unif}(\mathfrak{S}_D)} [\nu(u_i^-(\varphi)) - \nu(u_i^+(\varphi))], \end{aligned}$$

where \mathfrak{S}_D is the set of all permutations in D and u_i^+ , u_i^- return the set of all feature indices that precede i in the permutation π , in- and excluding i respectively. This expectation is approximated using Monte-Carlo sampling. By repeatedly sampling random permutations φ_ℓ the estimator is defined as $\hat{\phi}^\nu(i) := \frac{1}{L} \sum_{\ell=1}^L \nu(u_i^-(\varphi_\ell)) - \nu(u_i^+(\varphi_\ell))$. By updating all feature attribution scores, the efficiency property is maintained as $\sum_{i \in D} \nu(u_i^-(\varphi_\ell)) - \nu(u_i^+(\varphi_\ell)) = \nu(D) - \nu(\emptyset)$ for every permutation φ_ℓ .

SAGE Algorithm SAGE relies on the above permutation-based approximation method to estimate the Shapley values. The sampling of random permutations is thereby coupled with the approximation approach for $\hat{\nu}^f$.

Definition 2.1 (SAGE). Given data points $(x_n, y_n)_{n=1, \dots, N}$ and permutations $(\varphi_n)_{n=1, \dots, N}, \varphi_n \in \mathfrak{S}_D$ the SAGE estimator is defined as

$$\text{SAGE: } \hat{\phi}(i) := \frac{1}{N} \sum_{n=1}^N \mathcal{L}(\hat{f}^{u_i^-(\varphi_n)}(x_n), y_n) - \mathcal{L}(\hat{f}^{u_i^+(\varphi_n)}(x_n), y_n),$$

where $\hat{f}^S(x) := \frac{1}{M} \sum_{m=1}^M f(x^{(S)}, \tilde{x}_m^{(\bar{S})})$ and \tilde{x}_m are sampled from q by choosing \tilde{x}_m uniformly from the observed data points x_1, \dots, x_N .

The SAGE procedure is described in Algorithm 5. The permutation-sampling approach (Castro et al., 2009) ensures the

$$\text{SAGE efficiency: } \sum_{i \in D} \hat{\phi}(i) = \hat{\nu}^f(D).$$

It was shown that the SAGE estimator $\hat{\phi}(i)$ converges to $\phi^\nu(i)$ for $N \rightarrow \infty$ and $M \rightarrow \infty$ and that $\hat{\phi}(i)$ is asymptotically normal with variance reducing with order $\mathcal{O}(1/N)$

(Covert et al., 2020). The proofs rely on the assumption that the samples \tilde{x}_m are drawn from the true (conditional) distribution p . While SAGE provides efficient estimates of global FI, it is not well suited for an incremental learning task on a data stream that is possibly affected by concept drift. In Appendix D, we show an example (Figure 8) which illustrates that SAGE yields wrong importance scores if the underlying distribution is not static. As a remedy, we propose an incremental variant which can react to changing distributions.

3. Incremental Global Feature Importance

In the following, we consider a data stream, where at time t the observations $(x_0, y_0), \dots, (x_t, y_t)$ have been observed. On this data stream, a model f_t is incrementally learned over time by updating at $f_t \rightarrow f_{t+1}$ using the observation (x_t, y_t) . (Bahri et al., 2021; Losing et al., 2018) Our goal is to provide SAGE values alongside the incremental learning process using minimal resources. In general, the batch variant of SAGE is unable to handle shifting data distributions and model changes that can be caused by concept drift. In particular, in an online learning scenario, where the model is constantly adapting, huge changes in global FI scores can occur, as has been observed by Haug et al. (2022) and Fumagalli et al. (2022). To guarantee the reliability of the learned models, it is crucial to understand SAGE values over time. The main challenge in applying SAGE in an online learning scenario is that the model f_t , the data-generating random variables (X_t, Y_t) , and the sampling distribution q_t may change dynamically over time.

Sliding Window SAGE (SW-SAGE) A naive approach of computing SAGE values in an incremental manner is through repeated calculation within a sliding window (SW), which we denote as *SW-SAGE*. Applying SW-SAGE, necessitates storing all historical observations (x_t, y_t) for the last w (window length) observations, and recomputing the SAGE values from scratch based on the most up-to-date model f_t . The size w of the window has a profound effect on the resulting SAGE values. Choosing a large value for w , may increase the quality of the estimated SAGE values (larger sample), but can also lead to wrong importance scores, since the window contains outdated observations. Vice versa, a window size too small leads to a high variance. Yet, the high computational effort and the inability to reuse past results, because of the dynamic nature of f_t , strictly limits SW approaches in many scenarios, as discussed in Section 4.2. As a result, we propose a time-dependent version of the SAGE estimator, which we refer to as *incremental SAGE* (iSAGE).

Algorithm 1 Incremental SAGE

Require: stream $\{x_t, y_t\}_{t=1}^{\infty}$, feature indices $D = \{1, \dots, d\}$, model function f_t^D , loss function \mathcal{L} , and inner samples m

- 1: Initialize $\hat{\phi}^1 \leftarrow 0, \hat{\phi}^2 \leftarrow 0, \dots, \hat{\phi}^d \leftarrow 0$, and smoothed mean prediction $y_0 \leftarrow 0$
- 2: **for all** $(x_t, y_t) \in$ stream **do**
- 3: Sample π , a permutation of D
- 4: $S \leftarrow \emptyset$
- 5: $y_0 \leftarrow (1 - \alpha) \cdot y_0 + \alpha \cdot f(x_t)$ ▷ Update mean prediction
- 6: $\text{lossPrev} \leftarrow \mathcal{L}(y_0, y_t)$ ▷ Compute mean prediction loss
- 7: **for** $j = 1$ to d **do** ▷ Iterate over π
- 8: $S \leftarrow S \cup \{\pi[j]\}$
- 9: $y \leftarrow 0$
- 10: **for** $k = 1$ to m **do** ▷ Marginalize prediction with S
- 11: Sample $x_k^{(\bar{S})} \sim q(X^{(\bar{S})} \mid X^{(S)} = x^{(S)})$ ▷ marginal (Algorithm 2) or conditional (Algorithm 3)
- 12: $y \leftarrow y + f(x_t^{(S)}, x_k^{(\bar{S})})$
- 13: **end for**
- 14: $\bar{y} \leftarrow \frac{y}{m}$
- 15: $\text{loss} \leftarrow \mathcal{L}(\bar{y}, y_t)$
- 16: $\Delta \leftarrow \text{lossPrev} - \text{loss}$
- 17: $\hat{\phi}^{\pi[j]} \leftarrow (1 - \alpha) \cdot \phi^{\pi[j]} + \alpha \cdot \Delta$
- 18: $\text{lossPrev} \leftarrow \text{loss}$
- 19: **end for**
- 20: **end for**
- 21: **return** $\phi^1, \phi^2, \dots, \phi^d$

3.1. Incremental SAGE (iSAGE)

At each time step, we observe a sample (x_t, y_t) from the data stream, and our goal is to update the FI values using the current model f_t . We sample a random permutation φ_t to compute the marginal contribution for $i \in D$ as

$$\Delta_t(i) := \mathcal{L}(\hat{f}_t^{u_i^-(\varphi_t)}(x_t^{u_i^-(\varphi_t)}), y_t) - \mathcal{L}(\hat{f}_t^{u_i^+(\varphi_t)}(x_t^{u_i^+(\varphi_t)}), y_t),$$

where $\hat{f}_t^{(S)}$ is an approximation of the restricted model, further discussed below. These computations are then averaged over time, which yields the iSAGE estimator:

Definition 3.1 (iSAGE). The iSAGE estimator is recursively defined as

$$\text{iSAGE: } \hat{\phi}_t(i) = (1 - \alpha) \hat{\phi}_{t-1}(i) + \alpha \mathcal{L}(\hat{f}_t^{u_i^-(\varphi_t)}(x_t^{u_i^-(\varphi_t)}), y_t) - \mathcal{L}(\hat{f}_t^{u_i^+(\varphi_t)}(x_t^{u_i^+(\varphi_t)}), y_t),$$

where $\hat{\phi}_{t_0}(i) := \Delta_{t_0}(i)$ and $\alpha > 0$.

The iSAGE estimator retains the *efficiency* property with respect to the time-sensitive loss estimate

$$\hat{\nu}_t^{f_t}(S) := (1 - \alpha) \hat{\nu}_{t-1}^{f_{t-1}} + \underbrace{\alpha (\mathcal{L}(\hat{f}_t^{\emptyset}(x_t^{(\emptyset)}), y_t) - \mathcal{L}(\hat{f}_t^S(x_t^{(S)}), y_t))}_{\text{approximative reduction in loss at time } t}$$

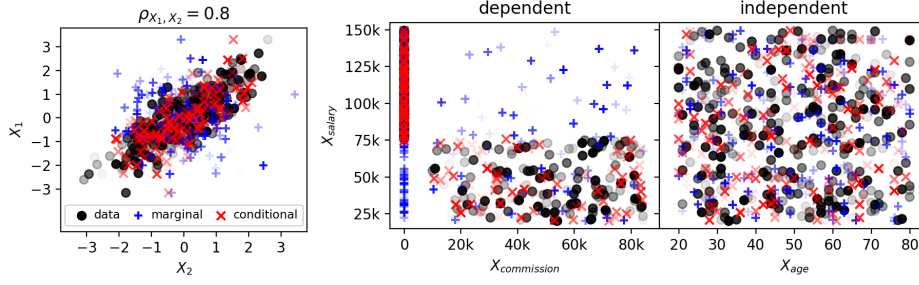


Figure 2: Conditional (red) and marginal (blue) feature removal strategies; The features follow the distributions $X_1 \sim \mathcal{N}(0, 1)$, $X_2 \sim \mathcal{N}(0, 1)$, $X_{\text{age}} \sim \text{unif}([20, 80])$, $X_{\text{salary}} \sim \text{unif}([20k, 150k])$, and $X_{\text{commission}} = \mathbf{1}(X_{\text{salary}} \leq 75k) \cdot Q$ with $Q \sim \text{unif}([10k, 75k])$.

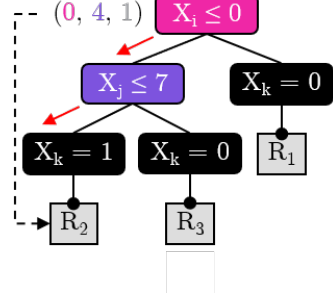


Figure 3: Illustration of the tree storage mechanism for a feature X_k and $\{X_i, X_j\}$. Each leaf links to a reservoir R_k .

with $\hat{\nu}_{t_0}^{f_{t_0}}(S) := \mathcal{L}(\hat{f}_{t_0}^{\emptyset}(x_{t_0}^{(\emptyset)}), y_{t_0}) - \mathcal{L}(\hat{f}_{t_0}^S(x_{t_0}^{(S)}), y_{t_0})$. The efficiency property reads as

$$\text{iSAGE efficiency: } \sum_{i \in D} \hat{\phi}_t(i) = \hat{\nu}_t^{f_t}(D).$$

Given the model f_t , the restricted model is again defined as $f_t^S(x^{(S)}) := \mathbb{E}_{\tilde{X} \sim p_t}[f_t(x^{(S)}, \tilde{X}_t)]$. In contrast to the batch scenario, the probability distribution p_t may change over time. We thus propose two choices of sampling distributions q_t , which can be used to approximate p_t in a dynamic learning environment.

3.2. Incremental Feature Removal Strategies

As mentioned in Section 2, SAGE is defined with the conditional distribution for p , yet approximates it with the marginal distribution q . In our view, different applications require different choices of q , and we propose two incremental approximations of each approach.

Marginal Distribution using Geometric Sampling. SAGE samples from the marginal distribution by uniformly choosing an observation from the given dataset. In an incremental learning scenario, this approach has significant drawbacks. First, access to the dataset is limited, as storing observations is traditionally considered to be infeasible for the whole data stream. Second, the marginal distribution may change over time, and it is, thus, beneficial to favor recent observations. The geometric sampling strategy, proposed by Fumagalli et al. (2022), accounts for both of these challenges. Geometric sampling maintains a reservoir of length L from which data points are sampled uniformly. The reservoir is updated at each time step with an incoming data point by uniformly replacing a data point from the reservoir. The geometric sampling strategy (fully initialized at time step $L := t_0$) chooses a previous observation from time r at time s with probability $L^{-1}(1 - L^{-1})^{s-r-1}$ for $r \geq L$, which clearly favors more recent observations. The

complete procedure is given in Algorithm 2. At any time t , geometric reservoir sampling requires a storage space of $\mathcal{O}(L)$ data points. It has been shown that the geometric sampling procedure is favorable in scenarios with concept drift compared to memory-efficient uniform sampling approaches, such as general reservoir sampling (Fumagalli et al., 2022).

Conditional Distribution using Incremental Decision Trees. The marginal distribution as a feature removal strategy can generate unrealistic observations when features are highly correlated, resulting in out-of-distribution evaluations of the model. This is illustrated in Figure 2, where marginal geometric sampling (blue) creates out of distribution samples in dependent or highly correlated settings. In some settings, it is inappropriate to evaluate the model outside the data manifold, and we propose an alternative approach that can incorporate feature dependence in the incremental sampling process.

To approximate the conditional distribution $p(X^{(\bar{S})}|X^{(S)} = x^{(S)})$, we rely on decision trees to compute conditional subgroups similar to Molnar et al. (2020) in the batch setting. For each feature $j \in D$, we train one decision tree that aims at predicting the current feature's value $x^{(j)}$ given $x^{(D \setminus j)}$ and storing the input samples in reservoirs at the corresponding leaf nodes. This procedure is illustrated in Figure 3. The observations reaching a corresponding leaf node are thus treated as *conditional subgroups*, from which observations are sampled to replace the feature's value in the imputation process. There are two key challenges when applying this approach in an incremental learning scenario. First, the distribution may change over time, which could require refactoring the decision tree structure and the subgroups over time. We solve this challenge by using an Hoeffding Adaptive Tree (HAT), a popular incremental variant of a decision tree (Hulten et al., 2001). The second challenge is that in contrast to computing PFI as Molnar et al. (2020), SAGE requires to approximate the conditional distribution

for *any* feature subset. A naive solution would be to train one decision tree for every possible feature subset, which quickly becomes infeasible for higher dimensions as it requires 2^d decision trees.

Instead, we propose to retain *one* incremental decision tree per feature, as illustrated in Algorithm 3. To approximate a feature’s value given a subset $S \subset D$ and an observation $x^{(S)}$, we traverse the decision tree using the values in $x^{(S)}$. If a decision node is based on a feature not present in S , then the path is determined by a random decision that uses the ratios of previously seen data points as probabilities for each child node. This methodology parallels the TreeSHAP approach of traversing decision trees (Lundberg et al., 2020). The process mimics the absence of arbitrary feature subsets while still relying on *one HAT per feature*. The reservoirs for each conditional subgroup are maintained using the geometric sampling procedure (Fumagalli et al., 2022). Conditional feature removal via HAT has a space complexity of $\mathcal{O}(d \cdot T^R \cdot L)$ where R refers to the HATs’ maximum tree depth, T is the maximum number of tree splits, and L is the size of the reservoir at each leaf node.

3.3. Approximation Guarantees

We presented an efficient algorithm to compute SAGE values incrementally. First, we show that the iSAGE estimator, similarly to its batch counterpart, approximates the SAGE values ϕ^{v^f} . We rely on the following assumption:

H0. We assume that $f \equiv f_t$ is a constant model and $(X, Y) \equiv (X_t, Y_t)$ a stationary data generating process.

In an incremental learning scenario H0 is approximately satisfied, if sufficiently many samples without concept drift have been observed.

Theorem 3.2. *Under H0, the iSAGE estimator $\hat{\phi}_t(i)$ approximates $\phi^{v^f}(i)$ for $M \rightarrow \infty$ and $t \rightarrow \infty$, given that samples are drawn according to the true conditional distribution p .*

Using Theorem 3.2 we now construct δ -confidence bounds on the approximation of the iSAGE estimator.

Theorem 3.3. *Under H0 and any confidence level $\delta > 0$ the iSAGE estimator approximates $\phi^{v^f}(i)$ up to an approximation error $\epsilon := (1 - \alpha)^{t - t_0 + 1} + \delta^{-\frac{1}{2}} \sigma(i) (\frac{\alpha}{2 - \alpha})^{\frac{1}{2}}$, i.e.*

$$\mathbb{P}(|\hat{\phi}_t(i) - \phi^{v^f}(i)| > \epsilon) < \delta,$$

where $\sigma^2(i) := \sigma_t^2(i) := \mathbb{V}[\Delta_t(i)]$.

For any $\delta > 0$, Theorem 3.3 ensures that the probability of $\hat{\phi}_t(i)$ differing more than ϵ from $\phi^{v^f}(i)$ is at most δ . To compute ϵ , we need an estimate for the unknown quantity $\sigma_t(i)$, which in practice may change over time. We propose

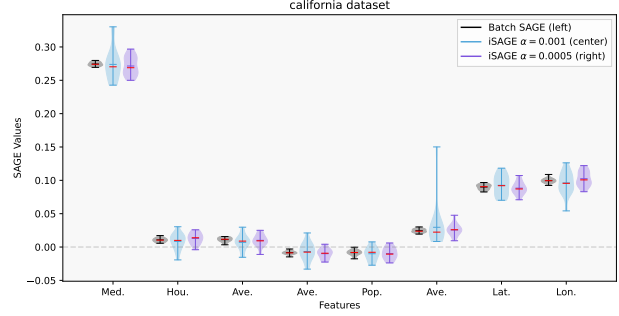


Figure 4: SAGE values (median in red) per feature of the *california* dataset for batch SAGE (left), and iSAGE (right).

to estimate the variance σ^2 according to

$$\hat{\sigma}_t^2(i) := (1 - \alpha)\hat{\sigma}_{t-1}^2(i) + \alpha(\Delta_t(i) - \hat{\phi}_t(i))^2,$$

with $\hat{\sigma}_{t_0}^2(i) := (\Delta_{t_0}(i) - \hat{\phi}_{t_0}(i))^2$, which constitutes a time-sensitive estimate of the variance. The δ -confidence bound at time t for $\hat{\phi}_t(i)$ is then computed as

$$\hat{\epsilon} := (1 - \alpha)^{t - t_0 + 1} + \sqrt{\frac{\hat{\sigma}_t^2(i)}{\delta} \frac{\alpha}{2 - \alpha}}.$$

4. Experiments

We conduct multiple experiments to validate our theoretical results and showcase the usefulness of our iSAGE estimator. First, we show that iSAGE leads to the same results as Covert et al. (2020)’s SAGE in static data scenarios validating Theorem 3.2 and 3.3. Second, we show how iSAGE can be efficiently applied in dynamic environments, yet still recover the correct SAGE values. Third, we illustrate the effect of choosing either one of the two feature removal strategies discussed in Section 3.2. As our iSAGE explanation technique is inherently model-agnostic, we train and evaluate our method on different incremental and batch models.²

4.1. Stationary Modeling Scenarios

We consider a static learning scenario, in which we compare iSAGE with Covert et al. (2020)’s original SAGE implementation for well-established benchmark batch datasets. The models are pre-trained and then explained. We apply Gradient Boosting Trees (GBTs) (Friedman, 2001), Light-GBM models (LGBM) (Ke et al., 2017), and neural networks (NNs). The original SAGE explanations are directly

²All model implementations are based on *scikit-learn* (Pedregosa et al., 2011), *River* (Montiel et al., 2021), and *torch* (Paszke et al., 2017). The data sets and streams are retrieved from *OpenML* (Feurer et al., 2021) and *River*. The data sets are described in detail in Appendix E.1. At acceptance, we will publicly provide our code on *github*. For review, it is appended to the supplement.

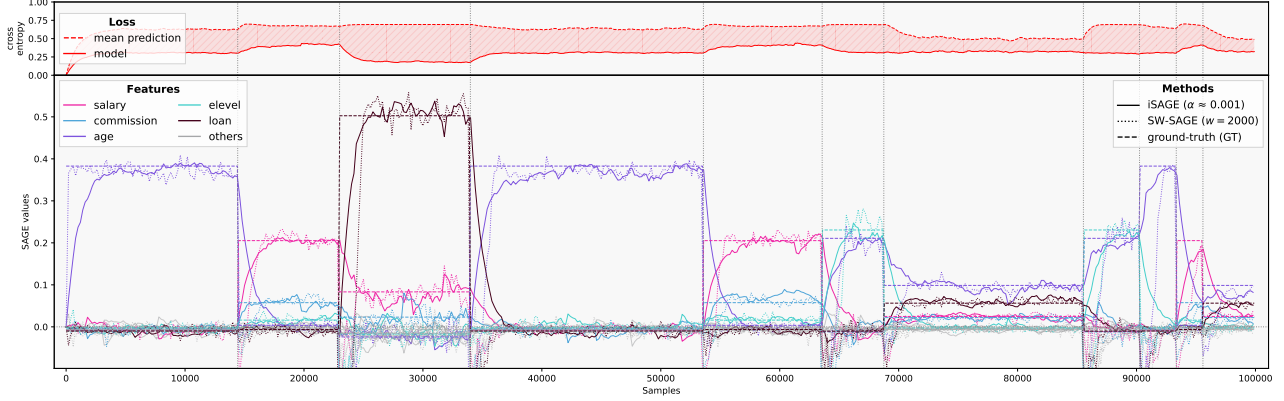


Figure 5: iSAGE (solid), SW-SAGE (dotted) and GT (dashed) values for an example GT stream. SW-SAGE is computed with a stride of 100 ($0.05 \cdot w$) resulting in an overhead 20 times higher than iSAGE.

Table 1: Approximation quality of iSAGE (inc_c) and SW-SAGE (SW_c) on synthetic GT data streams for 20 iterations (c denotes the factor of additional model evaluations compared to iSAGE). The complete results are given in Table 2.

scenario	size (w)	high		middle		low	
		500	1 000	500	1 000	500	1 000
MAE	inc_1	0.284	0.275	0.254	0.225	0.197	0.164
	(σ)	(0.075)	(0.067)	(0.080)	(0.077)	(0.052)	(0.041)
	SW_{20}	0.452	0.575	0.335	0.361	0.227	0.219
MSE	inc_1	0.034	0.038	0.027	0.027	0.015	0.013
	(σ)	(0.021)	(0.022)	(0.023)	(0.026)	(0.012)	(0.009)
	SW_{20}	0.283	0.420	0.191	0.320	0.049	0.078
	SW_1	0.248	0.462	0.183	0.399	0.061	0.080
		(0.198)	(0.413)	(0.200)	(0.792)	(0.067)	(0.079)

computed from the batch datasets. iSAGE experiences the datasets as a randomly shuffled data stream where the model is not updated incrementally. We run this explanation procedure 20 times and illustrate the SAGE values on the *california* example dataset in Figure 4. Figure 4 shows that iSAGE approximates SAGE in the static setting on average with a higher variance confirming Theorems 3.2 and 3.3. The higher variance as denoted in Theorem 3.3 is a direct result of the sampling procedure φ_{t_i} having no access to later data points ($t_j > t_i$) and the exponential smoothing mechanism controlled by α . iSAGE, thus, focuses more on recent samples, which is essential for non-stationary environments like incremental learning under potential drift.

4.2. Approximation Quality under Drift

In this experiment, we demonstrate the explanatory capabilities of iSAGE in a dynamic learning scenario. Conducting ground-truth (GT) experiments in an incremental learning setting where models change with every data point observed is computationally prohibitive. Moreover, it is not clearly defined what constitutes a GT online explanation, nor how a GT, SW-SAGE should be parameterized for real-world data streams with hidden drifts. Hence, we propose to conduct two distinct experimental setups to validate the explanatory benefits of iSAGE. First (1), we construct synthetic data streams with pre-trained models for which the GT SAGE values are pre-computed in a batch mode. Within the streams, we induce a sudden concept drift by randomly switching between the pre-trained models. We observe how differently parameterized SW-SAGE and iSAGE estimators approximate the pre-defined GT values. We measure the approximation quality in terms of MAE, MSE, and P@3. Second (2), we illustrate how iSAGE uncovers changes in real incremental learning scenarios where models are updated with every new observation. We apply different dynamic model classes. We incrementally train Adaptive Random Forests (ARFs) (Gomes et al., 2017) and HATs.

(1) Approximation quality with synthetic ground-truths. Based on the *agrawal* concepts (Agrawal et al., 1993), we construct different data streams with known ground-truth and pre-train ARF classifiers on each data stream for 20 000 samples³. We then create a batch SAGE explanation based on 25 000 additional samples, $m = 5$ inner samples, and cross-entropy loss. We construct a separate explanation data stream where we randomly switch between the pre-trained models and data generators. We create three scenarios with

³Further details and illustrations of the GT streams are given in Appendix E.3.2 and Figure 10.

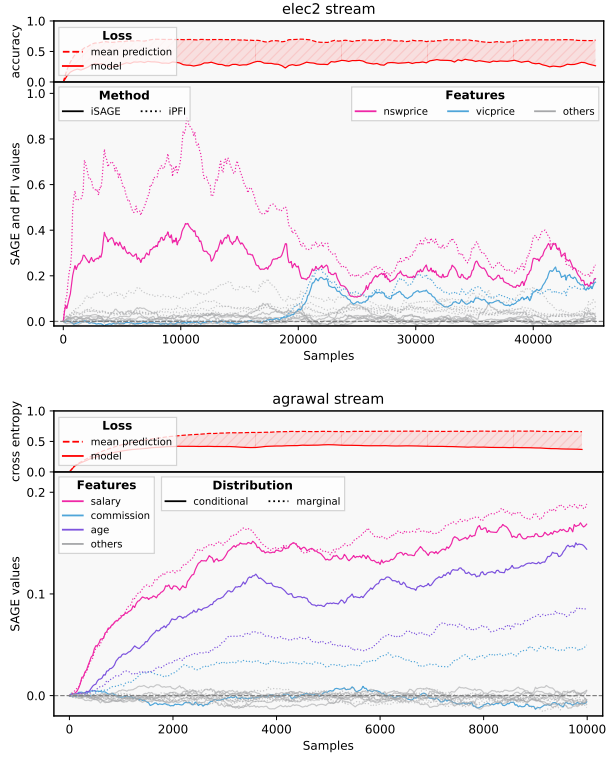


Figure 6: iSAGE and iPFI of an ARF on *elec2* (top) and iSAGE with *conditional* and *marginal* feature removal for an ARF on an *agrawal* stream (bottom)

varying degrees of concept drift (i.e. model switches); a *high*-, *middle*, and *low*-frequency scenario with on average 2 000, 5 000, and 10 000 samples in between a concept drift. In each scenario, we explain the underlying models with four different iSAGE and SW variants. The SW span $w_1 = 100$, $w_2 = 500$, $w_3 = 1000$, and $w_4 = 2000$ samples, and are computed with a stride (frequency) of $w_i/20$ samples. We couple iSAGE's α parameter with the window sizes $\alpha_i = 2/(w_i + 1)$ (Nahmias & Olsen, 2015). We repeat the complete experimental setup 20 times for each frequency scenario. The resulting approximation errors (MAE, MSE) are summarized in Table 2 and illustrated in Figure 5. Figure 5 shows, how iSAGE and SW-SAGE approximate the GT SAGE values. Independently of the substantially increased computational overhead (up to 20 times), SW-SAGE's approximation quality is substantially worse compared to iSAGE. In some scenarios, SW-SAGE reaches the GT values faster than iSAGE. Yet, in the important phases of change, SW-SAGE's estimates are substantially worse than iSAGE's (see Figure 11 for a detailed view). This is a result from SW-SAGE attributing equal weight to outdated observations included in the window after a concept drift and the current model f_t classifying the samples differently than the model before. iSAGE, however, smoothly changes between the different concepts.

(2) Dynamic explanations for incremental models We illustrate how iSAGE explanations can be used in real-world incremental learning scenarios to uncover hidden changes in black box incremental models. Therein, we compare iSAGE with incremental permutation feature importance (iPFI) (Fumagalli et al., 2022). Figure 6 explains the incremental learning procedure for an ARF classifier on the *elec2* data stream. Both methods detect similar feature importance rankings with varying absolute values, since iPFI, unlike SAGE, does not fulfill the efficiency axiom by distributing the explainable loss (difference between marginal and model loss in Figure 6) onto all features. Both methods correctly reveal the hidden changes in the model induced by the concept drift in the well-studied *elec2* (Harries, 1999). The concept drift, which stems from the *vicprice* feature not having any values in the first ≈ 20 000 observations, would be obfuscated by merely plotting the model performance. For additional experiments and a comparison with mean decrease in impurity (MDI) (Gomes et al., 2019) for an HAT classifier, we refer to the supplement material (E.3.3).

4.3. Marginal and Conditional Feature Removal

In the presence of dependent variables choosing one removal strategy over the other may have a profound effect on the FI values obtained. Hence, we propose two distinct sampling strategies for efficient feature removal in the incremental learning environment (Section 3.2). Figure 12 showcases how the iSAGE values differ with the conditional and marginal feature removal strategies with dependent data. An ARF model is trained and explained on the synthetic *agrawal* data stream. The synthetic classification function is defined in Section E.3.4.

In this stream the $X_{\text{commission}}$ feature ($X_{\text{com.}}$) directly depends on X_{salary} which is also illustrated in Figure 2. Whenever the *salary* of an applicant exceeds 75 000, no *commission* is given ($X_{\text{com.}} = 0$), and otherwise the commission is uniformly distributed ($X_{\text{com.}} \sim U(10\,000, 75\,000)$). Removing features based on the conditional data distribution instead of the marginal distribution yields different importance scores as illustrated in Figure 12. No significant importance is distributed to the $X_{\text{com.}}$ feature when features are removed through the conditional removal strategy. The importance is distributed onto the remaining two important features X_{salary} and X_{age} . However, when the marginal distribution is used to create removal values, the importance is also distributed to $X_{\text{com.}}$. The unrealistic feature values resulting from the marginal feature removal strategy uncover that the incremental model has picked up on the transient relationship between the target values and the feature $X_{\text{com.}}$.

5. Conclusion

We propose and analyze iSAGE, a novel and model-agnostic explanation procedure to compute global FI in dynamic environments. We show that iSAGE is an unbiased and consistent estimator of global FI based on Shapley values and construct δ confidence bounds. We further illustrate the efficacy of incremental explanations in multiple experiments on benchmark data sets and streams.

Still, approximating Shapley values remains a computationally challenging problem. Moreover, this approach does not address the problem of incrementally decomposing the interactions between features, which requires further investigation. Finally, the interaction between human users and incrementally created explanations derived from methods like iSAGE need to be vigorously evaluated to identify further research opportunities.

Acknowledgements

We gratefully acknowledge funding by the Deutsche Forschungsgemeinschaft (DFG, German Research Foundation): TRR 318/1 2021 – 438445824. The authors want to thank Rohit Jagtani for supporting the implementation and valuable discussions. The authors want to thank Gunnar König for valuable discussions and feedback.

References

Aas, K., Jullum, M., and Løland, A. Explaining individual predictions when features are dependent: More accurate approximations to shapley values. *Artificial Intelligence*, 298:103502, 2021. doi: 10.1016/j.artint.2021.103502.

Adadi, A. and Berrada, M. Peeking inside the black-box: A survey on explainable artificial intelligence (xai). *IEEE Access*, 6:52138–52160, 2018. doi: 10.1109/ACCESS.2018.2870052.

Agrawal, R., Imielinski, T., and Swami, A. Database Mining: A Performance Perspective. *IEEE Transactions on Knowledge and Data Engineering*, 5(6):914–925, 1993. doi: 10.1109/69.250074.

Atli, B. G. and Jung, A. Online feature ranking for intrusion detection systems. *CoRR*, abs/1803.00530, 2018. URL <https://arxiv.org/abs/1803.00530>.

Bahri, M., Bifet, A., Gama, J., Gomes, H. M., and Maniu, S. Data stream analysis: Foundations, major tasks and tools. *Wiley Interdisciplinary Reviews: Data Mining and Knowledge Discovery*, 11(3):e1405, 2021.

Barddal, J. P., Enembreck, F., Gomes, H. M., Bifet, A., and Pfahringer, B. Boosting decision stumps for dynamic feature selection on data streams. *Information Systems*, 83:13–29, 2019. doi: 10.1016/j.is.2019.02.003.

Breiman, L. Random Forests. *Machine Learning*, 45(1): 5–32, 2001.

Casalicchio, G., Molnar, C., and Bischl, B. *Visualizing the Feature Importance for Black Box Models*, volume 11051 of *Lecture Notes in Computer Science*, pp. 655–670. Springer International Publishing, Cham, 2019. ISBN 978-3-030-10924-0. doi: 10.1007/978-3-030-10925-7\40. URL <http://link.springer.com/10.1007/978-3-030-10925-7%5F40>.

Cassidy, A. P. and Deviney, F. A. Calculating feature importance in data streams with concept drift using online random forest. In *2014 IEEE International Conference on Big Data (Big Data)*, pp. 23–28, 2014. doi: 10.1109/BigData.2014.7004352.

Castro, J., Gómez, D., and Tejada, J. Polynomial calculation of the shapley value based on sampling. *Computers & Operations Research*, 36(5):1726–1730, 2009. doi: 10.1016/j.cor.2008.04.004.

Chen, H., Janizek, J. D., Lundberg, S. M., and Lee, S. True to the model or true to the data? *CoRR*, abs/2006.16234, 2020. URL <https://arxiv.org/abs/2006.16234>.

Clements, J. M., Xu, D., Yousefi, N., and Efimov, D. Sequential deep learning for credit risk monitoring with tabular financial data. *CoRR*, abs/2012.15330, 2020. URL <https://arxiv.org/abs/2012.15330>.

Covert, I., Lundberg, S. M., and Lee, S.-I. Understanding Global Feature Contributions With Additive Importance Measures. In *Advances in Neural Information Processing Systems 33 (NeurIPS 2020)*, pp. 17212–17223, 2020.

Covert, I., Lundberg, S. M., and Lee, S.-I. Explaining by Removing: A Unified Framework for Model Explanation. *Journal of Machine Learning Research*, 22(209):1–90, 2021.

Duckworth, C., Chmiel, F. P., Burns, D. K., Zlatev, Z. D., White, N. M., Daniels, T. W. V., Kiuber, M., and Boniface, M. J. Using explainable machine learning to characterise data drift and detect emergent health risks for emergency department admissions during covid-19. *Scientific Reports*, 11(1):23017, Dec 2021. doi: 10.1038/s41598-021-02481-y.

Fanaee-T, H. and Gama, J. Event labeling combining ensemble detectors and background knowledge. *Progress in Artificial Intelligence*, 2(2):113–127, 2014. doi: 10.1007/s13748-013-0040-3.

Feurer, M., van Rijn, J. N., Kadra, A., Gijsbers, P., Mallik, N., Ravi, S., Müller, A., Vanschoren, J., and Hutter, F. Openml-python: an extensible python API

for openml. *Journal of Machine Learning Research*, 22:100:1–100:5, 2021. URL <http://jmlr.org/papers/v22/19-920.html>.

Friedman, J. H. Greedy function approximation: A gradient boosting machine. *The Annals of Statistics*, 29(5):1189–1232, 2001.

Frye, C., Mijolla, D. d., Begley, T., Cowton, L., Stanley, M., and Feige, I. Shapley explainability on the data manifold. In *International Conference on Learning Representations*, 2021. URL <https://openreview.net/forum?id=OPyWRrcjVQw>.

Fumagalli, F., Muschalik, M., Hüllermeier, E., and Hammer, B. Incremental Permutation Feature Importance (iPFI): Towards Online Explanations on Data Streams. *CoRR*, abs/2209.01939, 2022. doi: 10.48550/arXiv.2209.01939. URL <https://doi.org/10.48550/arXiv.2209.01939>.

García-Martín, E., Rodrigues, C. F., Riley, G., and Grahn, H. Estimation of energy consumption in machine learning. *Journal of Parallel and Distributed Computing*, 134:75–88, 2019. doi: 10.1016/j.jpdc.2019.07.007.

Gomes, H. M., Bifet, A., Read, J., Barddal, J. P., Enembreck, F., Pfahringer, B., Holmes, G., and Abdessalem, T. Adaptive random forests for evolving data stream classification. *Machine Learning*, 106(9):1469–1495, 2017.

Gomes, H. M., Mello, R. F. d., Pfahringer, B., and Bifet, A. Feature scoring using tree-based ensembles for evolving data streams. In *2019 IEEE International Conference on Big Data (Big Data 2019)*, pp. 761–769, 2019.

Harries, M. Splice-2 comparative evaluation: Electricity pricing. Technical report, The University of South Wales, 1999.

Haug, J., Braun, A., Zürn, S., and Kasneci, G. Change detection for local explainability in evolving data streams. In *Proceedings of the 31st ACM International Conference on Information & Knowledge Management CIKM 2022*, pp. 706–716. ACM, 2022. doi: 10.1145/3511808.3557257.

Hulten, G., Spencer, L., and Domingos, P. Mining time-changing data streams. In *Proceedings of the seventh ACM SIGKDD international conference on Knowledge discovery and data mining (KDD 2001)*, pp. 97–106. ACM Press, 2001. doi: 10.1145/502512.502529.

Janzing, D., Minorics, L., and Blöbaum, P. Feature relevance quantification in explainable AI: A causal problem. In *The 23rd International Conference on Artificial Intelligence and Statistics (AISTATS 2020)*, volume 108 of *Proceedings of Machine Learning Research*, pp. 2907–2916. PMLR, 2020.

Ke, G., Meng, Q., Finley, T., Wang, T., Chen, W., Ma, W., Ye, Q., and Liu, T.-Y. Lightgbm: A highly efficient gradient boosting decision tree. In *Advances in Neural Information Processing Systems 30 (NeurIPS 2017)*, 2017.

Kohavi, R. Scaling up the Accuracy of Naive-Bayes Classifiers: A Decision-Tree Hybrid. In *Proceedings of International Conference on Knowledge Discovery and Data Mining (KDD 1996)*, pp. 202–207, 1996.

König, G., Molnar, C., Bischl, B., and Grosse-Wentrup, M. Relative feature importance. In *Proceedings of International Conference on Pattern Recognition*, pp. 9318–9325, 2021.

Losing, V., Hammer, B., and Wersing, H. Incremental online learning: A review and comparison of state of the art algorithms. *Neurocomputing*, 275:1261–1274, 2018. doi: 10.1016/j.neucom.2017.06.084.

Lundberg, S. M. and Lee, S.-I. A Unified Approach to Interpreting Model Predictions. In *Advances in Neural Information Processing Systems 30 (NeurIPS 2017)*, pp. 4768–4777, 2017.

Lundberg, S. M., Erion, G., Chen, H., DeGrave, A., Prutkin, J. M., Nair, B., Katz, R., Himmelfarb, J., Bansal, N., and Lee, S.-I. From local explanations to global understanding with explainable AI for trees. *Nature Machine Intelligence*, 2(1):56–67, 2020.

Molnar, C., König, G., Bischl, B., and Casalicchio, G. Model-agnostic feature importance and effects with dependent features - A conditional subgroup approach. *CoRR*, abs/2006.04628, 2020. URL <https://arxiv.org/abs/2006.04628>.

Montiel, J., Halford, M., Mastelini, S. M., Bolmier, G., Sourty, R., Vaysse, R., Zouitine, A., Gomes, H. M., Read, J., Abdessalem, T., and Bifet, A. River: machine learning for streaming data in python. *J. Mach. Learn. Res.*, 22:110:1–110:8, 2021. URL <http://jmlr.org/papers/v22/20-1380.html>.

Moro, S., Cortez, P., and Laureano, R. Using Data Mining for Bank Direct Marketing: An Application of the CRISP-DM Methodology. In *Proceedings of the European Simulation and Modelling Conference (ESM 2011)*, 2011.

Muschalik, M., Fumagalli, F., Hammer, B., and Hüllermeier, E. Agnostic explanation of model change based on feature importance. *KI - Künstliche Intelligenz*, 2022. doi: 10.1007/s13218-022-00766-6.

Nahmias, S. and Olsen, T. L. *Production and operations analysis*. Waveland Press, Illinois, 2015.

Paszke, A., Gross, S., Chintala, S., Chanan, G., Yang, E., DeVito, Z., Lin, Z., Desmaison, A., Antiga, L., and Lerer, A. Automatic differentiation in pytorch. In *Advances in Neural Information Processing Systems 30 (NeurIPS 2017) Workshop*, 2017.

Pedregosa, F., Varoquaux, G., Gramfort, A., Michel, V., Thirion, B., Grisel, O., Blondel, M., Prettenhofer, P., Weiss, R., Dubourg, V., Vanderplas, J., Passos, A., Cournapeau, D., Brucher, M., Perrot, M., and Duchesnay, E. Scikit-learn: Machine Learning in Python. *Journal of Machine Learning Research*, 12:2825–2830, 2011.

Ribeiro, M. T., Singh, S., and Guestrin, C. "Why Should I Trust You?": Explaining the Predictions of Any Classifier. In *Proceedings of International Conference on Knowledge Discovery and Data Mining, San Francisco*, pp. 1135–1144, 2016.

Schlùmmer, J. C. and Granger, R. H. Incremental learning from noisy data. *Machine Learning*, 1(3):317–354, 1986. doi: 10.1023/A:1022810614389.

Shapley, L. S. A Value for n-Person Games. In *Contributions to the Theory of Games (AM-28), Volume II*, pp. 307–318. Princeton University Press, 1953. ISBN 9781400881970. doi: 10.1515/9781400881970-018.

Ta, V.-D., Liu, C.-M., and Nkabinde, G. W. Big data stream computing in healthcare real-time analytics. In *Proceedings of International Conference on Cloud Computing and Big Data Analysis (ICCCBDA 2016)*, pp. 37–42, 2016. doi: 10.1109/ICCCBDA.2016.7529531.

Yuan, L., Pfahringer, B., and Barddal, J. P. Iterative subset selection for feature drifting data streams. In *Proceedings of the 33rd Annual ACM Symposium on Applied Computing*, pp. 510–517, 2018.

Zeiler, M. D. and Fergus, R. Visualizing and understanding convolutional networks. In *Computer Vision (ECCV 2014)*, volume 8689 of *Lecture Notes in Computer Science*, pp. 818–833. Springer, 2014. doi: 10.1007/978-3-319-10590-1_53.

Organization of the Supplement Material

The proofs of Theorem 3.2 and Theorem 3.3 are given in Section A. The confidence bounds derived in Theorem 3.3 are illustrated on a real-world data stream in Section B. Section C contains technical details about the two feature removal strategies. Section D contains Covert et al. (2020)'s original batch SAGE algorithm and illustrates the pitfalls of applying it without a proper incrementalization mechanism in a dynamic learning environment. Finally, Section E contains additional information about the data sets and streams, models and experimental setup used in Section 4. Section E also includes further experimental results.

A. Proof of Theorem 3.2 and Theorem 3.3

Theorem. Under H0 the iSAGE estimator $\hat{\phi}_t(i)$ approximates $\phi^{\nu^f}(i)$ for $M \rightarrow \infty$ and $t \rightarrow \infty$, given that samples are drawn according to the true conditional distribution p .

Proof. With $M \rightarrow \infty$ and sampling iid from the conditional distribution p the law of large numbers ensures that the approximation converges, i.e. $\hat{f}_t^S(x) \rightarrow f_t^S(x)$ for every t and S almost surely. Hence,

$$\begin{aligned} \mathbb{E}_{\varphi_t} [\mathbb{E}_{(X,Y)} [\Delta_t(i)]] &= \mathbb{E}_{\varphi_t} [\mathbb{E}_{(X,Y)} [\mathcal{L}(\hat{f}_t^{u_i^-(\varphi_t)}(x_t^{u_i^-(\varphi_t)}), y_t) - \mathcal{L}(\hat{f}_t^{u_i^+(\varphi_t)}(x_t^{u_i^+(\varphi_t)}), y_t)]] \\ &\stackrel{M \rightarrow \infty}{\rightarrow} \mathbb{E}_{\varphi_t} [\nu^{f_t}(u_i^-(\varphi_t)) - \nu^{f_t}(u_i^+(\varphi_t))] = \phi^{\nu^{f_t}}(i) = \phi^{\nu^f}(i), \end{aligned}$$

as $f \equiv f_t$. Then $\hat{\phi}_t(i)$ can be written as a weighted sum $\hat{\phi}_t(i) = \alpha \sum_{s=t_0}^t (1-\alpha)^{t-s} \Delta_s(i)$ and thus

$$\mathbb{E}[\hat{\phi}_t(i)] = \alpha \sum_{s=t_0}^t (1-\alpha)^{t-s} \mathbb{E}[\Delta_s(i)] = \phi^{\nu^f}(i) (1 - (1-\alpha)^{t-t_0+1}) \stackrel{t \rightarrow \infty}{\rightarrow} \phi^{\nu^f}(i).$$

□

Theorem. Under H0 and any confidence level $\delta > 0$ the iSAGE estimator approximates $\phi^{\nu^f}(i)$ up to an approximation error $\epsilon := (1-\alpha)^{t-t_0+1} + \delta^{-\frac{1}{2}} \sigma(\frac{\alpha}{2-\alpha})^{\frac{1}{2}}$, i.e.

$$\mathbb{P}(|\hat{\phi}_t(i) - \phi^{\nu^f}(i)| > \epsilon) < \delta.$$

Proof. Under H0 the variance of $\Delta_t(i)$ is constant and we denote $\sigma^2 := \mathbb{V}[\Delta_t(i)]$. Furthermore, for two time steps s, t the random variables $\Delta_s(i), \Delta_t(i)$ are independent. Hence,

$$\mathbb{V}[\hat{\phi}_t(i)] = \alpha^2 \sum_{s=t_0}^t (1-\alpha)^{2(t-s)} \mathbb{V}[\Delta_t(i)] \leq \sigma^2 \frac{\alpha}{2-\alpha}.$$

As observed in the proof of Theorem 3.2, we have $\mathbb{E}[\hat{\phi}_t(i)] - \phi^{\nu^f}(i) = (1-\alpha)^{t-t_0+1}$ and thus by Chebyshev's inequality

$$\begin{aligned} \mathbb{P}(|\hat{\phi}_t(i) - \phi^{\nu^f}(i)| > \epsilon) &\leq \mathbb{P}(|\hat{\phi}_t(i) - \mathbb{E}[\hat{\phi}_t(i)]| + (1-\alpha)^{t-t_0+1} > \epsilon) \\ &\leq \frac{\mathbb{V}[\hat{\phi}_t(i)]}{(\epsilon - (1-\alpha)^{t-t_0+1})^2} \leq \frac{\sigma^2 \frac{\alpha}{2-\alpha}}{(\epsilon - (1-\alpha)^{t-t_0+1})^2} \\ &\leq \delta. \end{aligned}$$

□

$$\text{iSAGE: } \hat{\phi}_t(i) := (1-\alpha) \cdot \hat{\phi}_{t-1}(i) + \alpha \cdot \mathcal{L}(\hat{f}_t^{u_i^-(\varphi_t)}(x_t^{u_i^-(\varphi_t)}), y_t) - \mathcal{L}(\hat{f}_t^{u_i^+(\varphi_t)}(x_t^{u_i^+(\varphi_t)}), y_t),$$

B. Confidence Bounds

Figure 7 illustrates iSAGE’s confidence bounds defined in Theorem 3.3. An incremental ARF model is trained and explained on the *elec* data stream. The iSAGE explanations are computed with $\alpha = 0.001$ and $m = 1$.

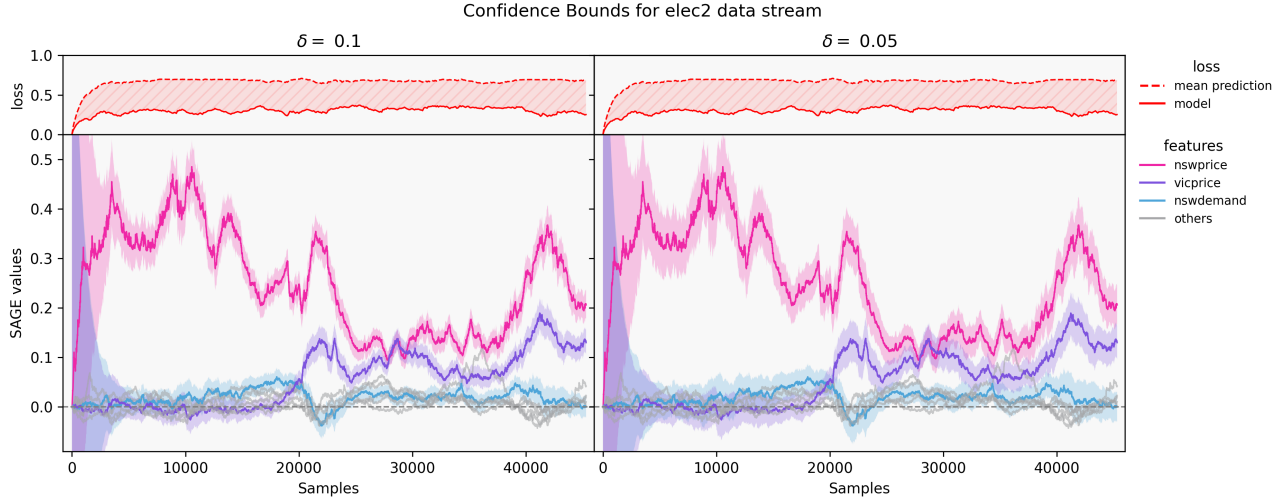


Figure 7: An ARF model is trained and explained on the *elec2* data stream ($\alpha = 0.001$ and $m = 1$). The confidence bounds of the point estimate are depicted with $\delta = 0.1$ (left) and $\delta = 0.05$ (right).

C. Feature Removal Strategies

We propose two distinct feature removal strategies for two different explanation needs. Notably approximating the marginal feature distribution (see Appendix C.1) and the conditional data distribution (see Appendix C.2) to sample replacement values to remove features from the model function (as described in Section 2 and Section 3.2).

C.1. Marginal Feature Removal with Reservoir Sampling

As described in Section 3.2, we apply geometric reservoir sampling to approximate a current estimate of the marginal feature distribution. The procedure in Algorithm 2 describes how new observations are stored in the reservoir. Sampling from the constructed reservoir is trivially defined by uniformly drawing a stored data point.

Algorithm 2 Updating the incremental geometric reservoir storage as described in (Fumagalli et al., 2022)

Require: stream $\{x_t^D\}_{t=1}^{\infty}$ feature indices $D \leftarrow \{1, 2, \dots, d\}$

- 1: Initialize reservoir $R \leftarrow \emptyset$ and number of seen samples with n
- 2: **for all** $x_t \in$ stream **do**
- 3: $n \leftarrow n + 1$
- 4: **if** $|R| \leq n$ **then**
- 5: $R \leftarrow R \cup x_t$
- 6: **else**
- 7: $i \leftarrow \text{RANDOMINTEGER}(0, |R|)$
- 8: $R \leftarrow R \setminus R[i]$
- 9: $R \leftarrow R \cup \{x_t\}$
- 10: **end if**
- 11: **end for**

▷ sample index to replace in R uniformly until $[0, |R|]$

C.2. Conditional Feature Removal with Incremental Decision Trees

As described in Section 3.2, we propose to train efficient, incremental decision tree models to more closely approximate the conditional data distribution. The procedure to train these incremental decision trees is given in Algorithm 3.

Algorithm 3 Updating the incremental trees storage mechanism for efficient conditional feature removal

Require: stream $\{x_t^D\}_{t=1}^{\infty}$ feature indices $D \leftarrow \{1, 2, \dots, d\}$

1: Initialize the tree h_0^i , its leafs $L_0^i \leftarrow \emptyset$, the data reservoirs $R_0^i \leftarrow \emptyset$, and a leaf-reservoir mapping $M^i(\cdot)$ for all $i \in D$

2: **for all** $x_t \in$ stream **do**

3: **for all** $i \in D$ **do**

4: $y_t^i \leftarrow x_t^i$

5: $x^r \leftarrow x_t^{D \setminus \{i\}}$ ▷ take rest of x as input features

6: $h_t^i \leftarrow \text{LEARN_ONE}(h_{t-1}^i, x^r, y_t^i)$ ▷ makes one incremental learning step with the remaining features as input

7: $L_t^i \leftarrow \text{GET_LEAFS}(h_t^i)$ ▷ traverses the tree and collects all leaf nodes

8: $R_t^i \leftarrow R_{t-1}^i \cup \text{INITIALIZE}(M^i(L_t^i \setminus L_{t-1}^i))$ ▷ initialize new reservoirs at new leaf nodes

9: $R_t^i \leftarrow R_t^i \setminus M^i(L_{t-1}^i \setminus L_t^i)$ ▷ delete outdated reservoirs

10: $l_t^i \leftarrow \text{PREDICT_LEAF}(h_t^i, x^{D \setminus i})$ ▷ get the leaf node associated with a prediction given the remaining features

11: $r_{t-1}^i \leftarrow M^i(l_t^i)$ ▷ get the reservoir associated with the leaf node

12: $r_t^i \leftarrow r_{t-1}^i \cup x_t$ ▷ update the reservoir with current sample

13: **end for**

14: **end for**

15: **return** all trees h_t^i and reservoirs R_t^i for $i \in D$

Algorithm 4 Leaf Traversal Procedure

1: **procedure** TRAVERSE(node: n , sample: x , features present: S)

2: Initialize sampling ratios $W \leftarrow \emptyset$

3: **if** n is split node **then**

4: **if** n splits on a feature present in S **then**

5: $c \leftarrow \text{GETNEXTCHILD}(x)$ ▷ make the split according to x

6: $n \leftarrow \text{TRAVERSE}(c, x)$

7: **return** n

8: **end if**

9: $C \leftarrow \text{GETCHILDREN}(n)$ ▷ get all children of n

10: **for all** nodes $c \in C$ **do**

11: $W \leftarrow W \cup \text{GETWEIGHT}(c)$ ▷ get weight of child in terms of how many samples have visited

12: **end for**

13: $c \leftarrow \text{SAMPLEWITHWEIGHT}(C, W)$ ▷ convert weights into probabilities and sample a child node accordingly

14: $n \leftarrow \text{TRAVERSE}(c, x)$

15: **return** n

16: **end if**

17: **return** n ▷ node n is a leaf node

18: **end procedure**

D. The Batch SAGE Algorithm

Algorithm 5 contains Covert et al. 2020’s original sampling-based SAGE algorithm. The algorithm’s notation is adjusted to fit into this paper’s mathematical notation. Figure 8 illustrates the pitfall of naively applying SAGE (as defined in Algorithm 5) in an incremental setting. The resulting importance values are incorrect because SAGE attributes equal weight onto each individual approximation step (in Lines 2 and 13 of Algorithm 5). Hence, older estimates that are no longer in-line with the real importance scores of a ever-changing model are given the same weight as more recent estimates.

Algorithm 5 Sampling-based approximation for SAGE values (Covert et al., 2020)

Require: data $\{x_i, y_i\}_{i=1}^N$, model f , loss function l , outer samples n , inner samples m

- 1: Initialize $\hat{\phi}^1 \leftarrow 0, \hat{\phi}^2 \leftarrow 0, \dots, \hat{\phi}^d \leftarrow 0$
- 2: $y_\emptyset \leftarrow \frac{1}{N} \sum_{i=1}^N f(x_i)$ ▷ Marginal Prediction
- 3: **for all** $(x_i, y_i) \in \text{data}$ **do**
- 4: Sample π , a permutation of D
- 5: $S \leftarrow \emptyset$
- 6: lossPrev $\leftarrow \mathcal{L}(y_\emptyset, y_i)$
- 7: **for** $j = 1$ to d **do**
- 8: $S \leftarrow S \cup \{\pi[j]\}$
- 9: $y \leftarrow 0$
- 10: **for** $k = 1$ to m **do**
- 11: Sample $x_k^{(\bar{S})} \sim q\left(X^{(\bar{S})} \mid X^{(S)} = x^{(S)}\right)$ ▷ In practice: $\mathbb{P}(X^{(\bar{S})})$
- 12: $y \leftarrow y + f(x_i^{(S)}, x_k^{(\bar{S})})$
- 13: **end for**
- 14: $\bar{y} \leftarrow \frac{y}{m}$
- 15: loss $\leftarrow l(\bar{y}, y^i)$
- 16: $\Delta \leftarrow \text{lossPrev} - \text{loss}$
- 17: $\hat{\phi}^{\pi[j]} \leftarrow \hat{\phi}^{\pi[j]} + \Delta$
- 18: lossPrev $\leftarrow \text{loss}$
- 19: **end for**
- 20: **end for**
- 21: **return** $\frac{\hat{\phi}^1}{n}, \frac{\hat{\phi}^2}{n}, \dots, \frac{\hat{\phi}^d}{n}$

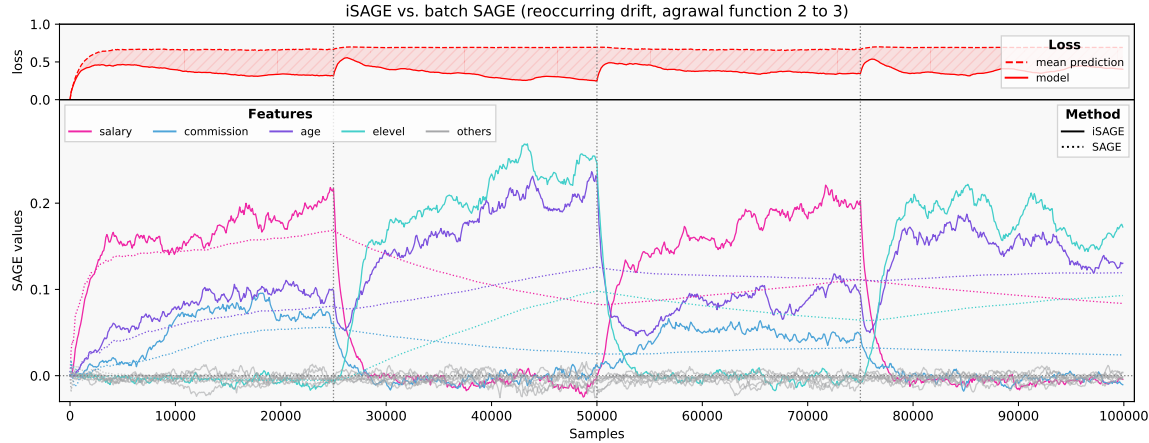


Figure 8: Static SAGE in Dynamic Learning Environment: The original SAGE (dash-dotted) is calculated in a dynamic, incremental learning scenario. Classical SAGE yields false importance scores when it is applied for a changing model, as it gives each importance score equal weight. iSAGE (solid) with $\alpha = 0.001$, and $m = 5$ is provided as a reference.

E. Experiments

This section contains additional information about the conducted experiments.

E.1. Data Set and Stream Descriptions

adult Binary classification dataset that classifies 48842 individuals based on 14 features into yearly salaries above and below 50k. There are six numerical features and eight nominal features. *adult* is a publicly available dataset (Kohavi, 1996).

bank Binary classification dataset that classifies 45211 marketing phone calls based on 17 features to decide whether they decided to subscribe a term deposit. There are seven numerical features and ten nominal features. *bank* is a publicly available dataset (Moro et al., 2011).

california Regression dataset containing 20640 samples of 8 numerical features with 1990 census information from the US state of California. The dataset is publicly available at https://www.dcc.fc.up.pt/~ltorgo/Regression/cal_housing.html

bike Regression dataset contains the hourly and daily count of rental bikes with information on weather. There are five numerical features and seven nominal features. *bike* is a publicly available dataset (Fanaee-T & Gama, 2014).

agrawal Synthetic data stream generator to create binary classification problems to decide whether an individual will be granted a loan based on nine features, six numerical and three nominal. There are ten different decision functions available. *agrawal* is a publicly available dataset (Agrawal et al., 1993).

stagger The *stagger* concepts makes a simple toy classification data stream. The synthetic data stream generator consists of three independent categorical features that describe the *shape*, *size*, and *color* of an artificial object. Different classification functions can be derived from these sharp distinctions. *stagger* is a publicly available dataset (Schlimmer & Granger, 1986).

elec2 Binary classification dataset that classifies, if the electricity price will go up or down. The data was collected for 45312 time stamps from the Australian New South Wales Electricity Market and is based on eight features, six numerical and two nominal. The data stream contains a well-documented concept drift in its *vicprice* feature in that the feature has no values apart from zero in all observations up to $\approx 20\,000$ samples. After that the *vicprice* feature starts having values different from zero. *elec2* is a publicly available dataset (Harries, 1999).

E.2. Summary of the Incremental Explanation Procedure

Algorithm 6 illustrates the simplified explanation procedure. For each data point in a data stream, the incremental model first predicts the current's data point target label y_t from x_t . This label is used for prequential evaluation of the model's performance and to calculate the model's loss at time t . Then, the model is explained with this data point to update the the current iSAGE estimate $\hat{\phi}_t$. After the explanation is updated the learning procedure is triggered for an incremental learning step.

Algorithm 6 Incremental explanation procedure

Require: stream $\{x_t, y_t\}_{t=1}^{\infty}$, model $f(\cdot)$, loss function $\mathcal{L}(\cdot)$

- 1: **for all** $(x_t, y_t) \in$ stream **do**
- 2: $\hat{y}_t \leftarrow f_t(x_t)$
- 3: $\hat{\phi}_t \leftarrow \text{explain_one}(x_t, y_t)$
- 4: $f_{t+1} \leftarrow \text{learn_one}(\mathcal{L}(\hat{y}_t, y_t))$
- 5: **end for**

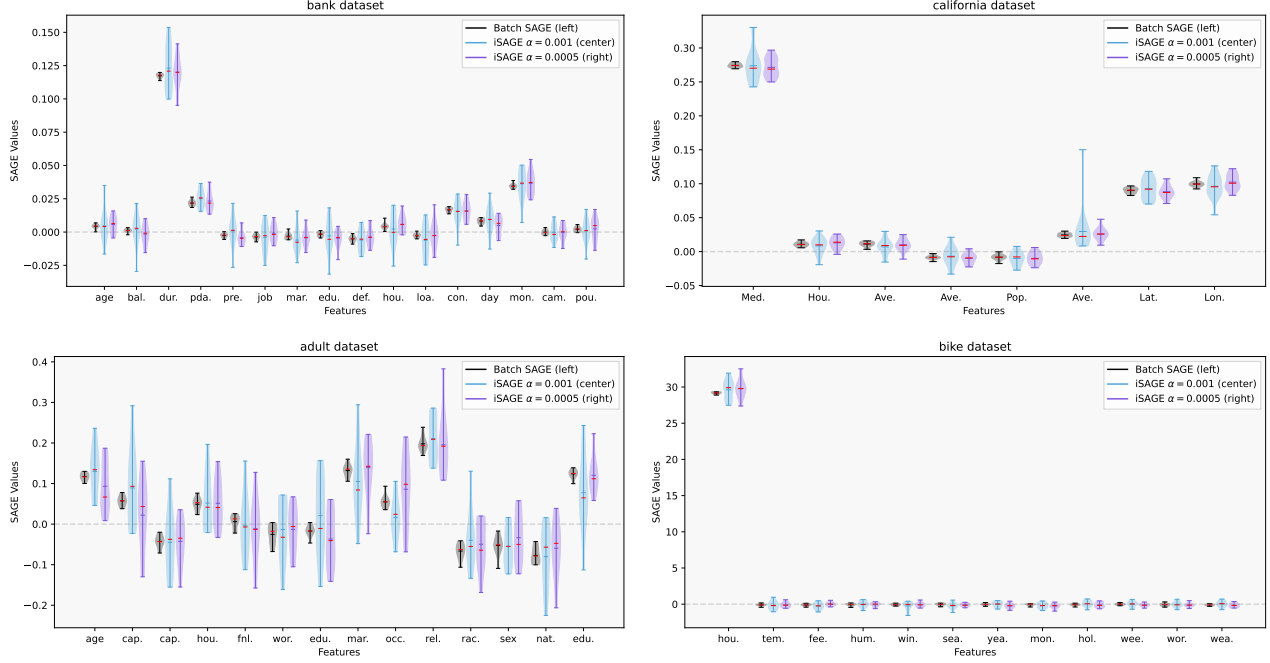


Figure 9: SAGE values in stationary data setting calculated with batch SAGE and iSAGE for the *bank* (top, left), *california* (top, right), *adult* (bottom, left), and *bike* (bottom, right) data sets.

E.3. Further Experimental Results

This subsection contains further results of the experiments conducted in Section 4. First, we present additional results for the stationary data setting. Second, we show examples of each synthetic GT scenario and provide further experimental results of different SW-SAGE window lengths and computational costs. Third, we show additional examples of iSAGE in real incremental learning scenarios from different data streams. Lastly, we provide the classification function to be learned omitted in Section 4.3.

E.3.1. APPROXIMATION QUALITY IN STATIC BATCH LEARNING SCENARIOS

Figure 9 contains SAGE values computed in a stationary data setting as described in 4.1. It shows the SAGE values for batch SAGE and iSAGE with $\alpha = 0.001$ and $\alpha = 0.0005$ for four datasets over multiple runs. For the *bank* dataset, a LightGBM model was trained with *max_iterations* set to 70, a *learning_rate* of 0.2 and a *tree_depth* of 15. The LightGBM was explained in 20 independent runs. For the *california* dataset, an ARF regressor was trained in an incremental manner with *n_models* set to 3 and explained in 20 independent runs. For the *adult* dataset, a batch random forest classifier was trained with *n_models* set to 15 and explained in 10 independent runs. The *bike* dataset, a HAT regressor was trained in an incremental manner and then explained in 20 independent runs.

E.3.2. APPROXIMATION QUALITY OF SYNTHETIC GROUND-TRUTH DATA STREAMS

In Figure 10 we present an exemplary data stream for each of the three scenarios of the synthetic GT experiments conducted in Section 4.2. Figure 10 shows how iSAGE and SW-SAGE approximate the pre-computed GT SAGE values for the pre-trained models. The runs in Figure 10 also show how SW-SAGE has a higher approximation error in times of change, whereas iSAGE gradually and smoothly switches between the concepts.

For each scenario and iteration run, we pre-train incremental models, pre-compute the SAGE values in a batch mode, randomly shuffle the models in a synthetic data stream. For each run, we pre-train six individual ARF classifiers (an ensemble with 3 HATs) on data generators based on the first six *agrawal* concepts (Agrawal et al., 1993). We train each ARF for 20 000 samples. After the pre-training, we compute the GT SAGE values according to Covert et al. (2020)'s original batch definition. Therein, we apply feature-removal according to the marginal feature distribution with $m = 10$. Then, we

create an artificial GT data stream by randomly switching between the different *agrawal* data generators yielding different data stream distributions. In each scenario, the probability of switching between the different pre-trained models is varied. For the setting with high-, middle, and low-frequency of changes, we set the probability of switching at each time (sample point) to $p_{\text{switch}} = 0.0005$, $p_{\text{switch}} = 0.0002$, and $p_{\text{switch}} = 0.0001$ respectively. On average, these probabilities result in a model change after 2 000, 5 000, and 10 000 samples for the high-, middle, and low-frequency scenarios.

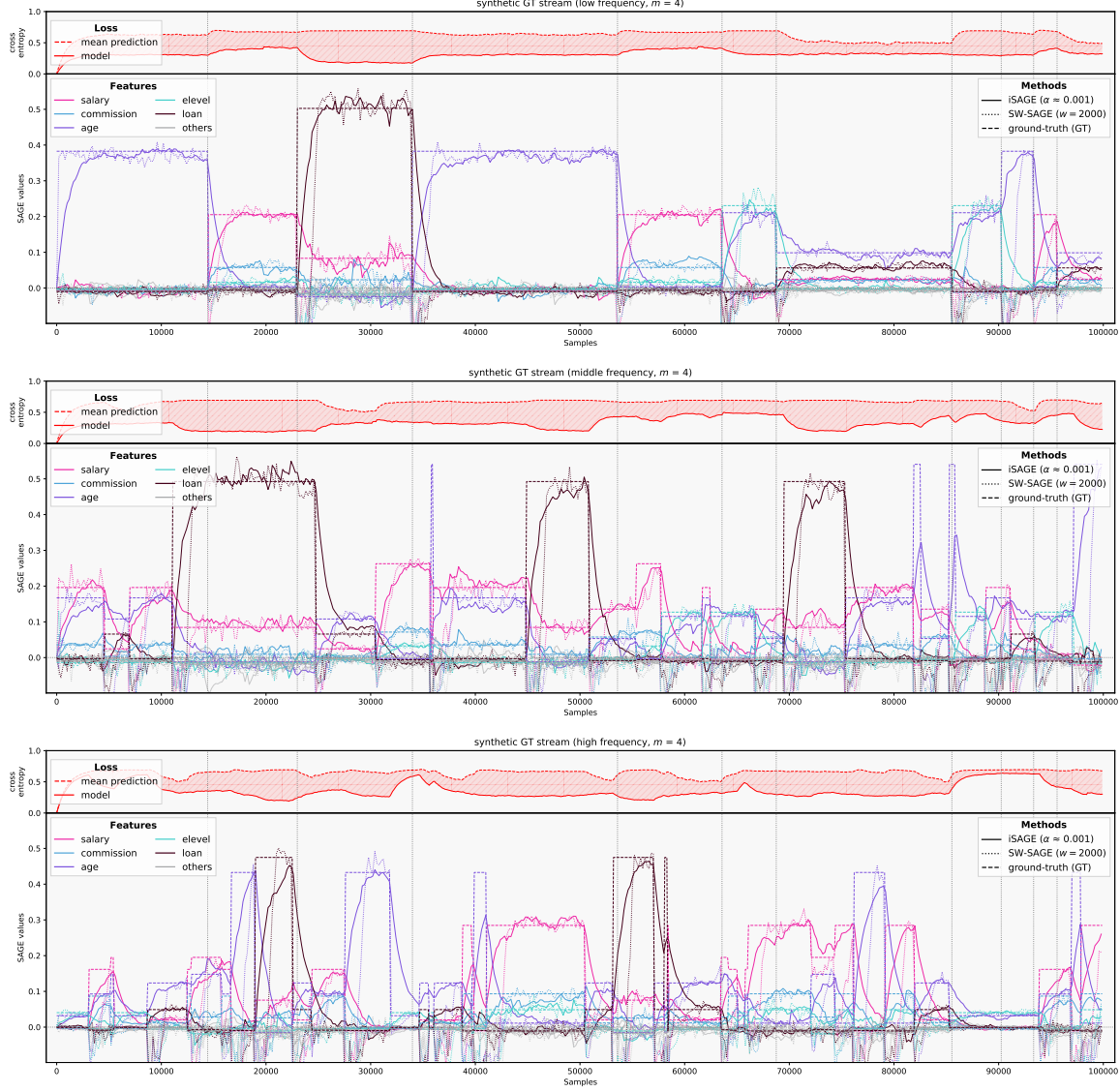


Figure 10: Three exemplary synthetic GT streams with iSAGE (solid), SW-SAGE (dotted), and the GT (dashed) for a low frequency (top), middle frequency (middle), and a high frequency (bottom) scenario. Presented are coupled iSAGE and SW-SAGE explanations with $\alpha \approx 0.001$, and $w = 2000$ and $m = 4$, respectively.

E.3.3. EXPLAINING INCREMENTAL MODELS

Next to the experiments in Section 4.2, we compare iSAGE with related FI methods; namely, incremental permutation feature importance (iPFI) (Fumagalli et al., 2022) and mean decrease in impurity (MDI) (Gomes et al., 2019). MDI, as a model-specific method, is only applicable on incremental decision trees. Hence, in Figure 12, we compute the three methods for a HAT on the *elec2* (Harries, 1999) real world data stream as an example. All methods correctly identify the two most important features.

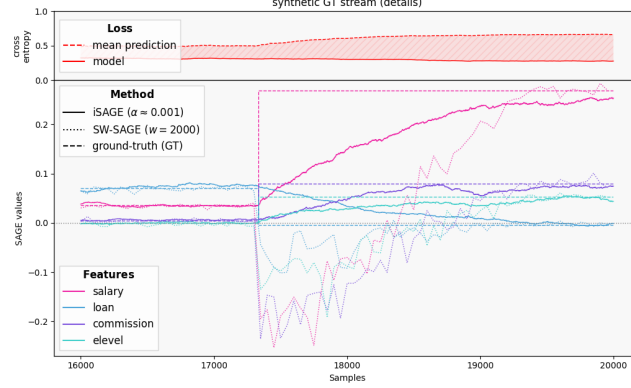


Figure 11: Detail view of a synthetic GT data stream. The models switch after 17 335 samples (different GT values). Before the switch, iSAGE and SW-SAGE approximate the GT well. Yet, after the switch, SW-SAGE recovers more slowly with a high approximation error.

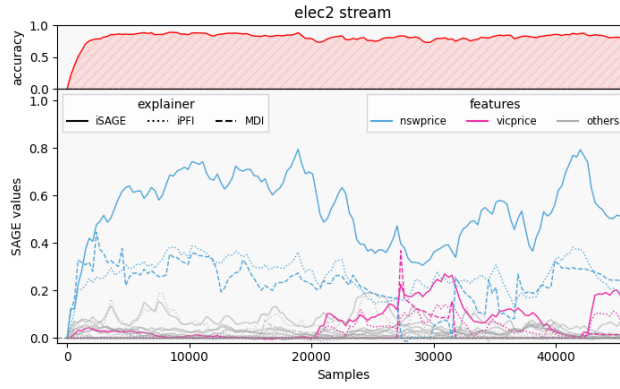


Figure 12: iSAGE, iPFI, and MDI for an HAT on *elec2*

E.3.4. CONDITIONAL AND MARGINAL FEATURE REMOVAL

Figure 14 shows how the iSAGE values differ when we apply the conditional feature removal mechanism compared to the marginal strategy. We conduct this experiment on an *agrawal* data stream with known feature dependencies and on the real-world data stream *elec2*. The classification function to be learned in on the *agrawal* stream is defined as

$$\begin{aligned}
 \text{class 1: } & ((X_{\text{age}} < 40) \wedge (50\,000 \leq X_{\text{salary}} \leq 100\,000)) \vee \\
 & ((40 \leq X_{\text{age}} < 60) \wedge (75\,000 \leq X_{\text{salary}} \leq 125\,000)) \vee \\
 & ((X_{\text{age}} \geq 60) \wedge (25\,000 \leq X_{\text{salary}} \leq 75\,000)).
 \end{aligned}$$

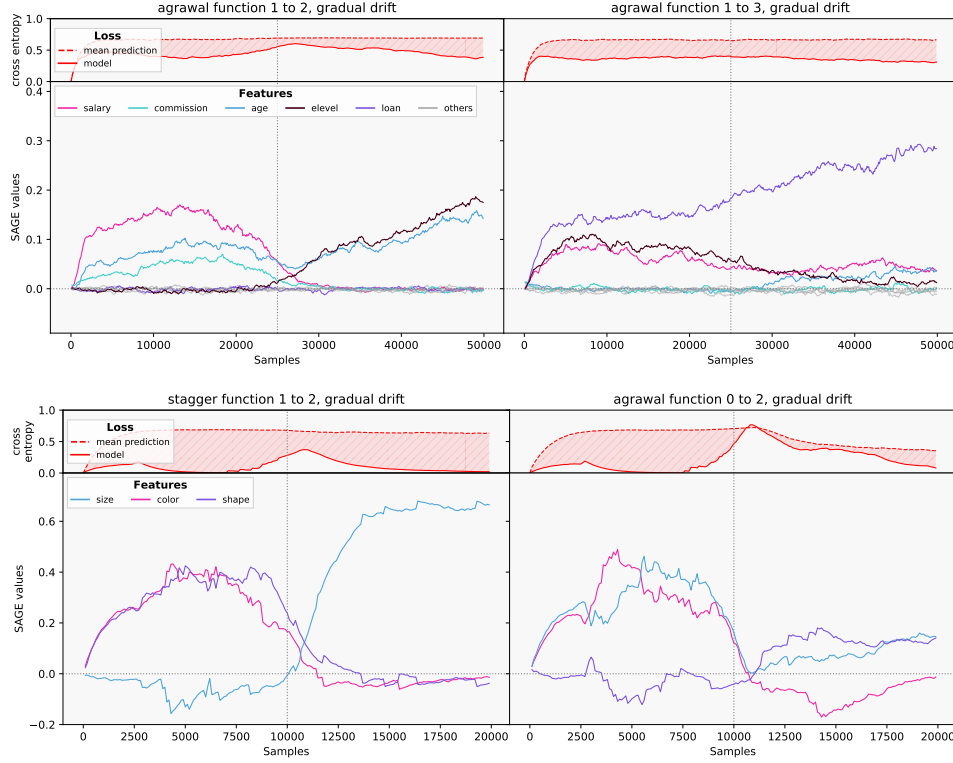


Figure 13: Two example cases of iSAGE explaining an ARF on an *agrwal* gradual concept drift stream (top) and a HAT on a *stagger* gradual concept drift stream (bottom)

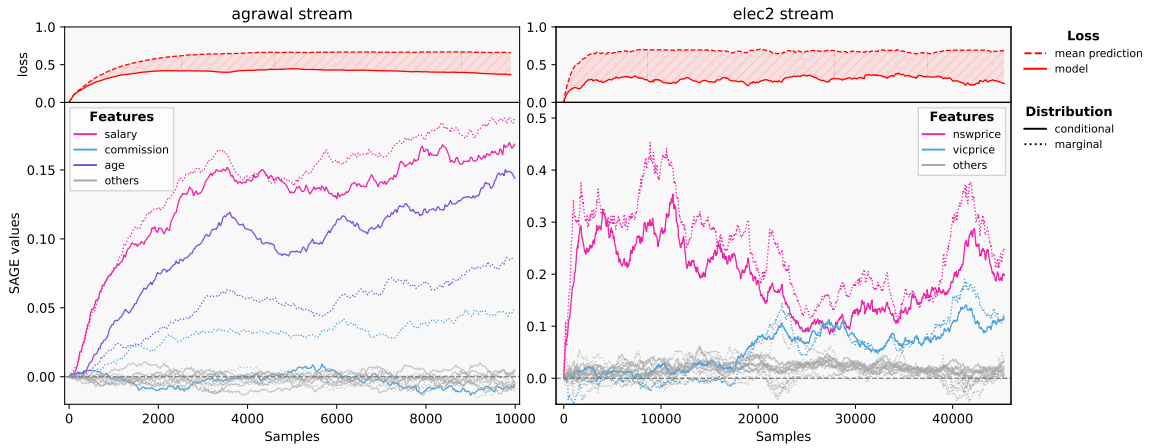


Figure 14: Comparison of iSAGE with conditional (dotted) and marginal (solid) for an *agrwal* stream with known feature dependencies (left) and *elec2* (right).

Table 2: Approximation quality of iSAGE and SW-SAGE on synthetic GT data streams for 20 iterations (inc_c denotes iSAGE and SW_c SW-SAGE with c denoting the factor of additional computational cost compared to iSAGE). (std. in brackets)

scenario		low				middle				high			
		100	500	1 000	2 000	100	500	1 000	2 000	100	500	1 000	2 000
MAE	inc ₁	.372 (.085)	.197 (.052)	.164 (.041)	.153 (.040)	.459 (.155)	.254 (.080)	.225 (.077)	.226 (.074)	.454 (.126)	.284 (.075)	.275 (.067)	.305 (.072)
	SW ₂₀	.384 (.092)	.227 (.057)	.219 (.060)	.261 (.085)	.492 (.172)	.335 (.111)	.361 (.121)	.480 (.175)	.505 (.139)	.452 (.130)	.575 (.176)	.811 (.249)
	SW ₁₀	.384 (.092)	.228 (.057)	.220 (.061)	.263 (.084)	.492 (.172)	.336 (.111)	.365 (.124)	.487 (.180)	.506 (.139)	.456 (.131)	.580 (.176)	.820 (.254)
	SW ₅	.384 (.092)	.230 (.058)	.221 (.061)	.264 (.081)	.494 (.173)	.338 (.112)	.371 (.130)	.494 (.184)	.508 (.140)	.462 (.132)	.592 (.184)	.839 (.257)
	SW ₂	.385 (.093)	.233 (.061)	.235 (.066)	.285 (.092)	.494 (.171)	.349 (.113)	.389 (.133)	.534 (.208)	.512 (.142)	.482 (.137)	.615 (.190)	.879 (.274)
	SW ₁	.386 (.092)	.244 (.064)	.246 (.070)	.306 (.098)	.495 (.171)	.364 (.121)	.426 (.160)	.566 (.216)	.519 (.143)	.506 (.148)	.670 (.214)	.921 (.345)
MSE	inc ₁	.057 (.042)	.015 (.012)	.013 (.009)	.015 (.011)	.103 (.105)	.027 (.023)	.027 (.026)	.034 (.034)	.094 (.066)	.034 (.021)	.038 (.022)	.051 (.027)
	SW ₂₀	.066 (.050)	.049 (.043)	.078 (.081)	.139 (.150)	.139 (.140)	.191 (.271)	.320 (.487)	.582 (.971)	.151 (.104)	.248 (.198)	.420 (.360)	.690 (.607)
	SW ₁₀	.065 (.050)	.049 (.044)	.080 (.086)	.137 (.148)	.139 (.139)	.189 (.266)	.325 (.501)	.596 (.035)	.152 (.105)	.250 (.198)	.422 (.360)	.690 (.612)
	SW ₅	.066 (.050)	.051 (.047)	.078 (.085)	.125 (.125)	.141 (.142)	.192 (.273)	.337 (.566)	.600 (.062)	.155 (.107)	.253 (.199)	.429 (.373)	.703 (.628)
	SW ₂	.065 (.047)	.051 (.048)	.088 (.106)	.137 (.145)	.137 (.133)	.176 (.226)	.326 (.466)	.652 (.249)	.156 (.104)	.259 (.211)	.432 (.399)	.713 (.644)
	SW ₁	.066 (.048)	.061 (.067)	.080 (.079)	.160 (.215)	.136 (.125)	.183 (.200)	.399 (.792)	.529 (.883)	.162 (.107)	.283 (.262)	.462 (.413)	.757 (.891)